microvascular resistance, and this increase is associated with the activation of PKC. Nondiabetic and diabetic rats had MCT values of 0.67 and 1.40 s, respectively (Fig. 3D). Oral treatment with 0.1, 1.0, and 10 mg/kg of LY333531 reduced MCT in the diabetic rats to 0.89, 0.84, and 0.87 s, respectively, but had no effect on nondiabetic rats. Again, the dose-response curve of LY333531 in ameliorating retinal MCT paralleled its inhibitory effect on PKC β activity (Fig. 2B). Our results demonstrate that in a rat model, an orally administered PKC β inhibitor can be effective in an isoenzyme-specific manner, without apparent toxicity, and can correct some of the vascular dysfunctions associated with diabetes mellitus. Hence, abnormal activation of PKC, in particular its β isoenzymes, may underlie some of these vascular complications of diabetes.

REFERENCES AND NOTES

1. Diabetes Control and Complication Trial Research Group, *N. Engl. J. Med.* **329**, 977 (1993).
2. T. Inoguchi *et al., Proc. Natl. Acad. Sci. U.S.A.* **89**, 11059 (1992).
3. Y. Nishizuka, *Science* **258**, 607 (1992).
4. H. Rasmussen, J. Forder, I. Kojima, A. Scriabine, *Biochem. Biophys. Res. Commun.* **122**, 776 (1984); C. Caramelo, P. Tsai, R. W. Schrier, *Biochem. J.* **254**, 625 (1988).
5. T. Shiba *et al., Am. J. Physiol.* **265**, E783 (1993).
6. P. A. Craven and F. R. DeRubertis, *J. Clin. Invest.* **83**, 1667 (1989).
7. T. Tamaoki *et al., Biochem. Biophys. Res. Commun.* **135**, 397 (1986); D. Toullec *et al., J. Biol. Chem.* **266**, 15771 (1991); E. Andrejauskas-Buchdunger and U. Regenass, *Cancer Res.* **52**, 5353 (1992).
8. M. R. Jirousek *et al., Bioorg. Med. Chem. Lett.*, in press.
9. F. E. Mitchell, R. M. Marais, P. J. Parker, *Biochem. J.* **261**, 131 (1989); S. Ohno, Y. Konno, Y. Akita, A. Yano, K. Suzuki, *J. Biol. Chem.* **265**, 6296 (1990); J. Zhang, L. Wang, J. Petrin, W. R. Bishop, R. W. Bond, *Proc. Natl. Acad. Sci. U.S.A.* **90**, 6130 (1993); J. Zhang, L. Wang, J. Schwartz, R. W. Bond, W. R. Bishop, *J. Biol. Chem.* **269**, 19578 (1994); E. M. Dutil, L. M. Keranen, A. A. DePaoli-Roach, A. C. Newton, *ibid.*, p. 29359.
10. P. Xia, R. M. Kramer, G. L. King, *J. Clin. Invest.* **96**, 733 (1995).
11. The serum half-life of LY333531 was ~6 hours. The main metabolite was a desmethylated product that in vitro was similar to LY333531 in potency and specificity of PKC β inhibition.
12. P. A. Craven, C. M. Davidson, F. R. DeRubertis, *Diabetes* **39**, 667 (1990); T. Inoguchi *et al., Am. J. Physiol.* **267**, E369 (1994); P. Xia *et al., Diabetes* **43**, 1122 (1994).
13. H. Ishii and G. L. King, unpublished data. PKC was partially purified from glomeruli of diabetic and nondiabetic rats (*2*), and PKC isoforms were measured by immunoblotting. PKC β_2 in the membranous fraction of diabetic rats was significantly increased (204 ± 43%) versus nondiabetic rats. No significant increases were observed with PKC isoenzymes α, δ, or ε in the same fraction.
14. T. H. Hostetter, H. G. Rennke, B. M. Brenner, *Am. J. Med.* **72**, 375 (1982).
15. M. P. O'Donnell, B. L. Kasiske, W. F. Keane, *FASEB J.* **2**, 2339 (1988).
16. C. E. Mogensen and C. K. Christensen, *N. Engl. J. Med.* **311**, 89 (1984).
17. M. Haneda *et al., Kidney Int.* **44**, 518 (1993); R. D. Hurst *et al., Diabetes* **44**, 759 (1995).
18. C. E. Mogensen, *N. Engl. J. Med.* **310**, 356 (1984); *Kidney Int.* **31**, 673 (1987).
19. S.-E. Bursell, A. C. Clermont, T. Shiba, G. L. King, *Curr. Eye Res.* **11**, 287 (1992).
20. The reaction mixture (250 μl) contained 30 μg of phosphatidylserine and 0.5 μg of DAG in 20 mM Hepes (pH 7.5), 10 mM $MgCl_2$, 100 μM EGTA (with or without 94 μM $CaCl_2$, depending on the PKC isoenzyme), histone (200 μg/ml) or myelin basic protein (250 μg/ml), compound in dimethyl sulfoxide (DMSO) or DMSO alone at four different concentrations, 30 μM ATP with γ-[^{32}P]ATP, and the PKC isoenzyme. Reaction time was 10 min at 30°C. Incubations were terminated with 500 μl of 25% trichloroacetic acid and 100 μl of bovine serum albumin (BSA) (1 mg/ml). The reaction mixture was filtered onto glass fiber mats with a Tom Tec filtration unit. Radioactivity was measured with a liquid scintillation counter.
21. H. Ohashi *et al., Regul. Pept.* **48**, 9 (1993).
22. LY333531 was synthesized by a cyclization reaction and converted to the dimethylamine derivative (*8*). (*S*)-1-*tert*-Butyldiphenylsilyloxy-2-(2-iodoethyloxy)-4-iodobutane was slowly added to a dimethylformamide slurry containing cesium carbonate and 3,4-bis(3,3′-indolyl)-1-methyl-pyrrole-2,5-dione. This isolated product was hydrolyzed and converted to the *NH*-maleimide with removal of the silyl protecting group. The resulting alcohol was converted to the mesylate and displaced with dimethyl amine to give the macrocyclic bis(indolyl)maleimide, LY333531.
23. A. Toker *et al., J. Biol. Chem.* **269**, 32358 (1994).
24. L. E. Heasley and G. L. Johnson, *J. Biol. Chem.* **264**, 8646 (1989); B. Williams and R. W. Schrier, *Diabetes* **41**, 1464 (1992).
25. I. Yasuda *et al., Biochem. Biophys. Res. Commun.* **166**, 1220 (1990).
26. The rats were anesthetized with thiopental sodium (50 mg/kg intraperitoneal). Catheters were then surgically inserted in the left carotid artery (for blood sampling), the left jugular vein (for infusion), and the urinary bladder (for collection of urine). Inulin (0.6%) and PAH (1.5%) in normal saline were infused at a rate of 6.0 ml/hour for 30 min, followed by a sustained infusion of 2.0 ml/hour throughout the experiment. After 60 min, two clearance studies (each 30 min) were performed in succession. The concentrations of inulin and PAH were measured by the anthrone method [W. H. Waugh, *Clin. Chem.* **23**, 639 (1977)] and the calorimetric technique [H. W. Smith, N. Finkelstein, L. Aliminosa, B. Crawford, M. Grabor, *J. Clin. Invest.* **24**, 388 (1945)], respectively. GFR and RPF were determined by inulin and PAH clearance, respectively, and the filtration fraction was calculated from the ratio of GFR to RPF.
27. Enzyme-linked immunosorbent assay (ELISA) plates were coated with 50 μl of sheep antibody to rat albumin immunoglobulin G (IgG) (10 μg/ml) at 4°C overnight and blocked with 100 μl of 1% BSA for 1 hour at 37°C. The plates were incubated with 50 μl of standard rat albumin or urine samples and then with 50 μl of peroxidase-conjugated sheep antibody to rat albumin IgG for 1 hour at 37°C. Finally, the reaction was started by incubation with 100 μl of 0.11 M Na_2HPO_4 and 0.04 M citric acid (pH 5.5) containing *o*-phenylenediamine dihydrochloride (1 mg/ml) and 0.05% hydrogen peroxide. After 2 min, the reaction was terminated by adding 100 μl of 3M H_2SO_4, and absorbance at 492 nm was measured with a spectrophotometer. The assay range was 3 to 250 ng/ml, and the intra- and inter-assay coefficients of variation were 2.4% and 6.5%, respectively.

28. Supported by National Eye Institute grant NEI-05110-11 and Diabetes and Endocrinology Research Center grant NIDDK-36836, and partially supported by Lilly Pharmaceutical, Inc. We thank J. Davis and K. Kalter for help with the in vitro kinase assays and L. Balmat for excellent secretarial assistance.

14 September 1995; accepted 13 March 1996

A Mouse Model of Familial Hypertrophic Cardiomyopathy

Anja A. T. Geisterfer-Lowrance, Michael Christe, David A. Conner, Joanne S. Ingwall, Frederick J. Schoen, Christine E. Seidman, J. G. Seidman*

A mouse model of familial hypertrophic cardiomyopathy (FHC) was generated by the introduction of an $Arg^{403} \rightarrow Gln$ mutation into the α cardiac myosin heavy chain (MHC) gene. Homozygous $\alpha MHC^{403/403}$ mice died 7 days after birth, and sedentary heterozygous $\alpha MHC^{403/+}$ mice survived for 1 year. Cardiac histopathology and dysfunction in the $\alpha MHC^{403/+}$ mice resembled human FHC. Cardiac dysfunction preceded histopathologic changes, and myocyte disarray, hypertrophy, and fibrosis increased with age. Young male $\alpha MHC^{403/+}$ mice showed more evidence of disease than did their female counterparts. Preliminary results suggested that exercise capacity may have been compromised in the $\alpha MHC^{403/+}$ mice. This mouse model may help to define the natural history of FHC.

FHC is an autosomal dominant condition characterized by unexplained ventricular hypertrophy with myocyte and myofibrillar disarray. Affected individuals typically experience shortness of breath, angina, and palpitations, but many are asymptomatic. Sudden death, heart failure, and stroke are the most serious consequences of the disease (*1*, *2*). Molecular genetic studies have demonstrated that mutations in the β cardiac MHC can cause FHC (*2*, *3*). However, FHC is clinically diverse even among affected family members who share the same β cardiac MHC mutation (*4*). For example, some affected individuals die during childhood, whereas others survive into their sixth to seventh decade (*1*, *2*). The mechanisms by which mutations in the β cardiac MHC cause hypertrophic cardiomyopathy, and the roles of physical activity, environment, and modifying genes in the clinical heterogeneity of the disease, are poorly understood.

A missense mutation, $Arg^{403} \rightarrow Gln$

(R403Q), in the β cardiac MHC gene causes a severe form of FHC; 50% of individuals with this mutation die by age 45 (*2*). We introduced the R403Q missense mutation into exon 13 of the mouse α cardiac MHC gene. This isoform is highly homologous to human β cardiac MHC [92% identical overall; 100% identical for 30 amino acids flanking residue 403 (*5*)] and is preferentially expressed in the adult mouse heart (*6*). We used the "hit and run" technique (*7*) to produce embryonic stem (ES) cells that carried the missense mutation on one allele (designated $\alpha MHC^{403/+}$ ES cells) (Fig. 1). $\alpha MHC^{403/+}$ ES cells were injected into mouse blastocysts, and the resultant chimeras were bred to obtain $\alpha MHC^{403/+}$ and $\alpha MHC^{403/403}$ mice.

Genotypes of mice were ascertained by Southern (DNA) blot analyses and restriction enzyme digestion of polymerase chain reaction (PCR)–amplified tail DNA (Fig. 1, B and C). Heterozygous mice bearing the mutant allele were viable, reproduced normally, and lacked overt symptoms (*8*). Homozygous mice ($\alpha MHC^{403/403}$) were live-born and had normal gross cardiac anatomy but uniformly died by day 7. The ratio of α and β cardiac MHC isoforms in the cardiac ventricle was assessed by polyacrylamide gel analysis of partially purified cardiac sarcomeres (*9*). The amounts of α and β cardiac MHC were the same in 6-day-old wild-type, $\alpha MHC^{403/+}$, and $\alpha MHC^{403/403}$ mouse hearts, which showed that the mutant polypeptide was stable in cardiac myocytes and was incorporated into sarcomeres (*8*).

Hearts from 5-week-old $\alpha MHC^{403/+}$ mice and wild-type littermates had similar gross anatomy (*8*). By 15 weeks, the hearts of some $\alpha MHC^{403/+}$ mice, but no wild-type mice, exhibited left atrial enlargement (Fig. 2A). Left atrial enlargement was present in 7 of 11 male versus 2 of 12 female $\alpha MHC^{403/+}$ mice at 15 weeks, and 7 of 7 male versus 6 of 18 female $\alpha MHC^{403/+}$ mice at 30 weeks ($P < 0.02$). Left atrium–body weight ratios were significantly greater in $\alpha MHC^{403/+}$ mice than in wild-type mice ($P < 0.02$; $\alpha MHC^{403/+}$ left atrium weight = 0.0073 ± 0.0028 g, wild-type left atrium weight = 0.0037 ± 0.0011 g). In contrast, total heart–body weight ratios or left ventricle–body weight ratios were not different between 40-week-old mutant and wild-type mice.

Cardiac histology was examined in wild-type and $\alpha MHC^{403/+}$ mice killed at ages 5, 15, and 30 weeks (Table 1). Histology was normal in wild-type mice of all ages (Fig. 3, C and F) and in 5-week-old mutant mice (*10*). Myocardial sections from 15-week-old $\alpha MHC^{403/+}$ mice exhibited disarray, hypertrophy, and injury (Fig. 3A) and interstitial fibrosis (Fig. 3D). Myocardial sections of 30-week-old $\alpha MHC^{403/+}$ mice exhibited the classic histopathology of human FHC: hypertrophied myocytes with large hyperchromatic nuclei and marked myocardial fiber disarray (Fig. 3B). Moderate diffuse interstitial fibrosis (Fig. 3E) and focal replacement granulation tissue were also observed in sections from 30-week-old mutant mice. The histologic changes became more pronounced with age and appeared more consistently in males than in females. Three of 10 female $\alpha MHC^{403/+}$ mice (two 15 weeks old, one 31 weeks old) showed no histologic abnormalities, but all male $\alpha MHC^{403/+}$ mice exhibited myocyte disarray. Significant myocyte hypertrophy, injury, and fibrosis were found more often in older $\alpha MHC^{403/+}$ mice than in 15-

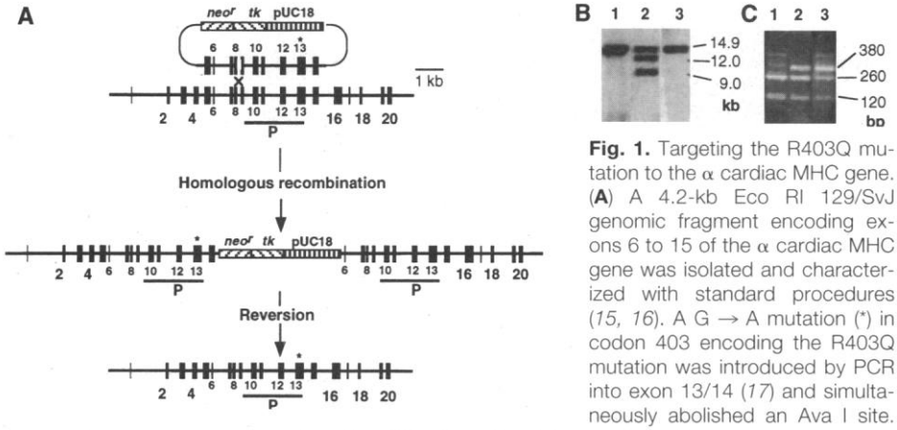

Fig. 1. Targeting the R403Q mutation to the α cardiac MHC gene. (**A**) A 4.2-kb Eco RI 129/SvJ genomic fragment encoding exons 6 to 15 of the α cardiac MHC gene was isolated and characterized with standard procedures (*15, 16*). A G → A mutation (*) in codon 403 encoding the R403Q mutation was introduced by PCR into exon 13/14 (*17*) and simultaneously abolished an Ava I site. The targeting construct was introduced into ES cells and homologous recombinants were selected as described (*18, 19*). Targeted ES cells were grown in FIAU-containing media to select for revertant cells bearing the R403Q mutation in the α cardiac MHC gene without the *tk* or *neo^r* genes (*20*). Fragment P was used as a probe in Southern blot analyses. (**B**) Southern blot analyses of ES cells. ES cell DNA was digested with Dra I (*21*) and hybridized to probe P. Lane 1, wild-type (WT) ES cells; exon 13/14 is encoded on a 14.9-kb Dra I fragment. Lane 2, targeted ES cells [probe P detects three fragments: a 14.9-kb fragment derived from the WT allele and two fragments (9 and 12 kb) derived from the new allele]. Lane 3, targeted and reverted ES cells; WT genomic structure is restored. (**C**) Mutation analysis of ES cells. Exon 13/14 of ES cells was amplified (*22*), digested with Ava I, and fractionated on an agarose gel. Lane 1, WT ES cells; lane 2, targeted ES cells (the mutated exon 13/14 lacks an Ava I site); lane 3, targeted and reverted ES cells that are heterozygous and contain the mutated and normal exon 13/14.

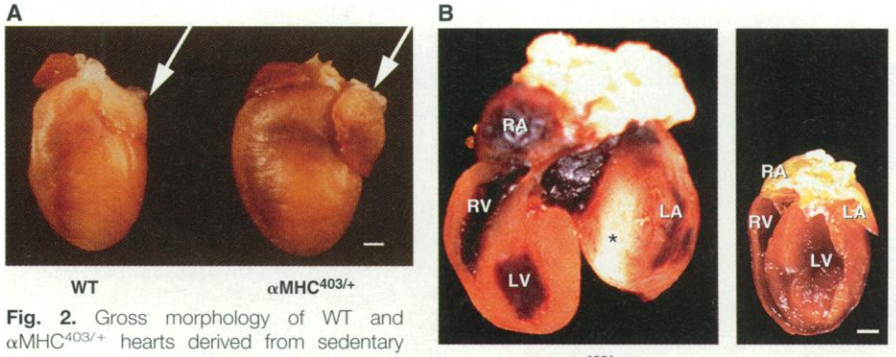

Fig. 2. Gross morphology of WT and $\alpha MHC^{403/+}$ hearts derived from sedentary and exercised mice. (**A**) Enlargement of the left atrium (arrow) is present in the sedentary $\alpha MHC^{403/+}$ mouse heart (right) but not the sedentary WT littermate heart (left). (**B**) Coronal section of hearts from exercised $\alpha MHC^{403/+}$ and WT mice. RA, right atrium; RV, right ventricle; LA, left atrium; LV, left ventricle. Left panel: The sudden-death $\alpha MHC^{403/+}$ mouse heart had fresh clot in all chambers and an organized thrombus (*) in the markedly enlarged LA. Note the asymmetric hypertrophy of the LV (*14*). Right panel: Normal cardiac anatomy was present in the WT mouse that completed 7 weeks of the swimming protocol. Scale bars, 1 mm.

A. A. T. Geisterfer-Lowrance, M. Christe, D. A. Conner, J. G. Seidman, Howard Hughes Medical Institute and Department of Genetics, Harvard Medical School, 200 Longwood Avenue, Boston, MA 02115, USA.
J. S. Ingwall, Department of Medicine, Brigham and Women's Hospital, 75 Francis Street, Boston, MA 02115, USA.
F. J. Schoen, Department of Pathology, Brigham and Women's Hospital, 75 Francis Street, Boston, MA 02115, USA.
C. E. Seidman, Howard Hughes Medical Institute, Brigham and Women's Hospital, 75 Francis Street, Boston MA 02115, USA.
*To whom correspondence should be addressed.

week-old αMHC$^{403/+}$ mice.

To assess the consequences of the αMHC^{403} mutation in cardiac function, we measured left ventricular pressures and cardiac outputs from isolated, perfused working hearts (*11*) of 5- and 15-week-old wild-type and mutant mice. The maximum left ventricular pressures generated by mutant and wild-type mice were similar; however, the profiles of their pressure curves differed significantly (Fig. 4A). During ventricular relaxation, time-dependent change in pressure was continuous in all wild-type mice ($n > 100$) but was discontinuous in all mutant mice studied ($n = 3$, age 5 weeks; $n = 7$, age 15 weeks). This discontinuity in pressure reduction produced an abnormal upward deflection in tracings that represented the rate of change of pressure (dP/dt, Fig. 4A). Moreover, the duration of relaxation (T_r) was longer in mutant mice than in wild-type mice (Fig. 4) ($P < 0.001$; $T_r = 0.046$ s for wild-type mice, $T_r = 0.060$ s for αMHC$^{403/+}$ mice). Cardiac function was also assessed by determining cardiac output at different preload pressures and after-load resistances (Fig. 4B). Cardiac output was less in 15-week-old αMHC$^{403/+}$ mice than in wild-type mice ($P < 0.01$) (Fig. 4B). Cardiac output was also less in 5-week-old mutant mice than in wild-type mice under conditions of high filling pressure or aortic resistance (*12*).

Humans with FHC can experience serious life-threatening events with vigorous exercise (*13*). To determine the impact of exercise on the αMHC$^{403/+}$ mice, we trained five mutant and five wild-type mice to swim. Each mouse swam twice daily during the 7-week exercise protocol; on the first day, the sessions were 10 min each, and their duration increased by 10 min per day to a maximum of 90 min per session, which was maintained for the remainder of the protocol. Five wild-type and three mutant mice tolerated the exercise protocol; they spontaneously groomed and fed immediately after swimming. Two αMHC$^{403/+}$ mice did not tolerate exercise; one died suddenly while swimming (2.5 weeks into protocol), and one survived swimming but was consistently lethargic for protracted periods after exercise. The heart from the sudden-death αMHC$^{403/+}$ mouse (Fig. 2B, left) was grossly enlarged and showed thrombus in the dilated left atrium, mild right ventricular hypertrophy, and marked asymmetric left ventricular hypertrophy (*14*). In contrast, the heart from a wild-type swimmer (Fig. 2B, right) was normal.

Mutant αMHC$^{403/+}$ mice provide a genetic model of human FHC. Analysis of these mice demonstrated that if the sarcomere contains 50% R403Q myosin, car-

Table 1. Histologic abnormalities of αMHC$^{403/+}$ hearts. Histologic specimens from αMHC$^{403/+}$ and wild-type littermates were prepared as in Fig. 3 and were scored, without knowledge of genotype, by an experienced cardiac pathologist (F.J.S.). Findings in mutant mice included myocyte hypertrophy (+, present; blank, absent) and myocyte disarray, myocyte injury and inflammation, and fibrosis (+, mild; ++, moderate; +++, severe; blank, none). Locations of disarray: 1, left ventricular free wall; 2, posterior left and right ventricular junction; 3, interventricular septum; 4, right ventricular free wall; 5, diffuse.

Mouse number	Age (weeks)	Sex	Myocyte hypertrophy	Myocyte disarray	Location	Myocyte injury	Fibrosis
1961	15	F					
1963	15	F					
1970	15	F		+	1		
1986	15	F		+	2		
1960	15	M	+	++	1, 3	++	++
1965	15	M		+	5		
1967	15	M		+	3	+	+
1971	15	M		+	2		
1467	30	F	+	+	1		
1471	30	F					+
1492	31	F	+	++	1, 3		+
1493	31	F					
1499	31	F	+	++	1, 2, 3, 4		+
1500	31	F	+	+	1		
1423	30	M		+	2, 3		
1482	31	M	+	++	1, 2, 3	+	++
1485	31	M		++	1		++
1495	31	M	+	+++	1, 2, 3		+
1498	31	M	+	++	1, 2, 3	++	+
1717	31	M		+	1, 2		

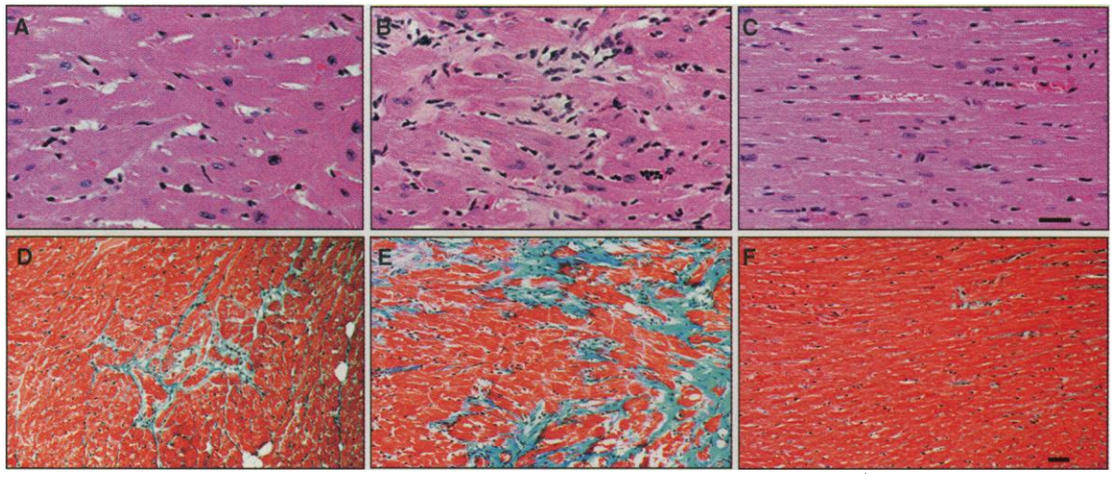

Fig. 3. Comparison of myocardial histology in mutant and WT mice. Fifteen-week-old (**A**) and 30-week-old (**B**) male αMHC$^{403/+}$ mice have myocyte hypertrophy and disarray that are absent in WT male mice (**C**). Progressive fibrosis, shown by collagen staining (blue) in 15-week-old (**D**) and 30-week-old (**E**) αMHC$^{403/+}$ mice, is absent in WT mice (**F**). Fixed hearts were cut transversely at the midventricular level. The basal portion was embedded in paraffin; sections were cut from the transected surface at 4 to 5 μm and stained with hematoxylin and eosin (H&E) stain for overall morphology. The apical portion was embedded in glycolmethacrylate; sections were cut at 2 μm and stained with Masons' trichrome (MT) stain for collagen. Sections were stained with H&E (A to C) or with MT (D to F). Scale bars, 100 μm.

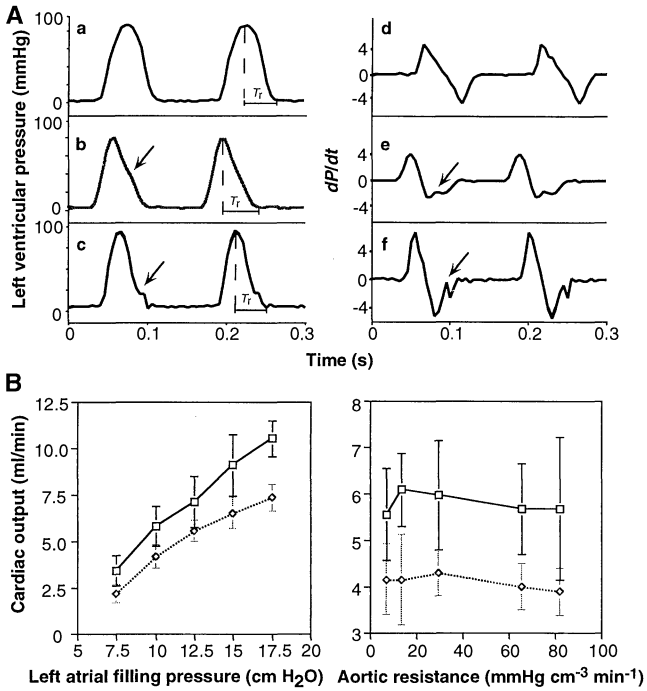

Fig. 4. (**A**) Left ventricular pressures in isolated working hearts of WT and αMHC$^{403/+}$ mice (*23*). Pressure tracings from WT mice (a) did not show the altered pressure wave form present in αMHC$^{403/+}$ mice [5 weeks old, (b); 15 weeks old, (c)] (arrows). The difference in left ventricular pressures was more easily visualized as the first derivative of pressure (*dP/dt*); again, tracings from WT hearts (d) were different from those obtained from mutant hearts [5 weeks old, (e); 15 weeks old, (f)] (arrows). (**B**) Cardiac outputs from isolated working hearts of WT and αMHC$^{403/+}$ mice. Outputs from 15-week-old mice were calculated as the sum of pulmonary artery (containing only coronary flow) and aortic effluents. Outputs from seven mutant hearts (◇) and six WT hearts (□) were measured. Left panel, variable filling pressures with a fixed resistance of 29 mmHg cm^{-3} min^{-1}; right panel, variable resistance with a constant filling pressure of 10 cm of H_2O. Differences were significant ($P < 0.01$) at each filling pressure and aortic resistance.

diac function is abnormal but compatible with life. If the sarcomere contains 100% R403Q myosin, the animal dies. Moreover, these mice exhibited the same cardiac histopathology and pathophysiology observed in human FHC. The mouse model provides definitive evidence for the genetic basis of FHC and demonstrates that cardiac dysfunction is the primary response to the R403Q myosin mutation. Because 5-week-old αMHC$^{403/+}$ mice had reduced cardiac output without histologic or morphologic abnormalities, we suggest that altered mechanical properties in the mutant sarcomere directly caused abnormal cardiac function. The compromised exercise capacity observed in two of five αMHC$^{403/+}$ mice probably resulted from factors such as reduced cardiac output, nonuniformity of ventricular relaxation or increased chamber stiffness (or both), and impedance to atrial emptying. Histopathology and morphologic abnormalities were age-dependent and occurred after the development of hemodynamic abnormalities. Myocyte disarray was an early cellular response to this mutation and typically preceded the development of myocyte hypertrophy; myocyte injury and replacement fibrosis generally appeared late.

A mouse model for FHC enables assessment of the impact of background genotype and physical activity on phenotype. We have demonstrated that both of these factors affect the clinical manifestations of FHC. Because male mutant mice were affected at an earlier age than were females, and because the differences between male and female inbred mice are genetically programmed, we conclude that modifying genes critically influence the phenotypic expression of the R403Q myosin mutation. Further elucidation of the impact of exercise, other environmental influences, and modifying genes on disease expression should help to direct the clinical management of FHC in humans. Ultimately, these mice may provide insights into the mechanisms and causes of cardiac remodeling and may help to define therapeutic targets for FHC and other cardiomyopathies.

REFERENCES AND NOTES

1. J. Wynne and E. Braunwald, in *Heart Disease: A Textbook of Cardiovascular Medicine*, E. Braunwald, Ed. (Saunders, Philadelphia, 1992), pp. 1394–1450.
2. C. E. Seidman and J. G. Seidman, in *Molecular Cardiovascular Medicine*, E. Haber, Ed. (Scientific American, New York, 1995), pp. 193–210.
3. H. Watkins, J. G. Seidman, C. E. Seidman, *Hum. Mol. Genet.* **4**, 1721 (1995); H. Watkins *et al.*, *Nature Genet.* **11**, 434 (1995).
4. B. J. Maron, R. O. Bonow, R. O. Cannon III, M. B. Leon, S. E. Epstein, *N. Engl. J. Med.* **316**, 780 (1987); W. McKenna *et al.*, *Am. J. Cardiol.* **47**, 532 (1981).
5. T. Jaenicke *et al.*, *Genomics* **8**, 194 (1990); A. A. T. Geisterfer-Lowrance, unpublished results.
6. L. A. Leinwand, R. E. K. Fournier, B. Nadal-Ginard, T. B. Shows, *Science* **221**, 766 (1983).
7. P. Hasty, R. Ramírez-Solis, R. Krumlauf, A. Bradley, *Nature* **350**, 243 (1991); V. Valancius and O. Smithies, *Mol. Cell. Biol.* **11**, 1402 (1991).
8. A. A. T. Geisterfer-Lowrance, M. Christe, C. E. Seidman, J. G. Seidman, unpublished data.
9. R. J. Solaro, D. C. Pang, F. N. Briggs, *Biochim. Biophys. Acta* **245**, 259 (1971).
10. M. Christe, F. J. Schoen, C. E. Seidman, J. G. Seidman, unpublished data.
11. M. E. Christe *et al.*, *Am. J. Physiol.* **267**, H2050 (1994).
12. M. Christe and J. S. Ingwall, unpublished data.
13. B. J. Maron, W. C. Roberts, S. E. Epstein, *Circulation* **65**, 1388 (1992).
14. The subaortic interventricular septum and left ventricular free wall were 2.5 and 3 times as thick, respectively, as the apical wall (0.9 to 1.1 mm).
15. Exons 13 and 14 are fused into a single exon (designated exon 13 in Fig. 1) in mouse α and β cardiac MHC genes (A. A. T. Geisterfer-Lowrance, C. E. Seidman, J. G. Seidman, unpublished data).
16. J. H. Weis and T. Quertermous, in *Current Protocols in Molecular Biology*, F. M. Ausubel *et al.*, Eds. (Wiley, New York, 1994), chap. 5.
17. The primers used for introducing the R403Q mutation were 5′-GCCTGTGTCACCCTC**A**GGTGAAGGTGGGGAACGAGTATGTC-3′ and 5′-TTCCCCACCTTCACC**T**GAGGGTGACACAGGCCCTTGAGCAG-3′.
18. B. A. Hendrickson *et al.*, *J. Exp. Med.* **182**, 1905 (1995); W. Zhang *et al.*, *ibid.* **183**, 1 (1996). The construct was linearized with Eco RV (located in intron 8 of the α cardiac MHC gene), introduced into C1 ES cells by electroporation, and grown in selective media.
19. The targeting construct and the endogenous α cardiac MHC gene underwent homologous recombination in about 1 of 50 neomycin-resistant cells (A. A. T. Geisterfer-Lowrance, M. Christe, D. A. Conner, J. S. Ingwall, F. J. Schoen, C. E. Seidman, J. G. Seidman, data not shown).
20. About 1 in 10^6 targeted ES cells grew in fialuridine (FIAU)–containing media. The desired intrachromosomal recombination event occurred more frequently in cells that were grown for only a few hours without G418 before selection in FIAU (A. A. T. Geisterfer-Lowrance, M. Christe, D. A. Conner, J. S. Ingwall, F. J. Schoen, C. E. Seidman, J. G. Seidman, data not shown).
21. Because the pUC18 sequences in the targeting construct contained three Dra I sites, the Dra I fragment encoding the endogenous exon 13/14 of the α cardiac MHC gene was shorter after the insertion of the targeting construct.
22. Exon 13/14 was amplified with primers 5′-GGACAAAGGAATGGAGGTACTGAAA-3′ and 5′-CTGATGGTCTGAGTGGGTAGGTGAG-3′.
23. Working heart preparations were made with the use of a modified procedure described previously for rat hearts (*11*). Mouse hearts were perfused with Krebs-Henseleit buffer (containing 2 mM Ca^{2+} and 10 mM glucose) and studied in a system that was designed to allow for rapid changes in volume (left atrial filling pressure) and pressure (aortic resistance) loading. Left ventricular and aortic pressures were monitored by means of in-dwelling cannulae coupled to Statham P23 pressure transducers and were recorded on a Maclab A/D system. Hearts were paced at 6.8 Hz (400 beats/min). Cardiac function was assessed during volume loads of 7.5, 10, 12.5, 15, and 17.5 cm of H_2O by changing the height of the filling reservoir relative to the heart; aortic resistance was held at 29 mmHg cm^{-3} min^{-1}. Functional measurements were also recorded at various pressure loads. With left atrial filling pressure held at 10 cm of H_2O, aortic outflow was directed through one of five segments of polyethylene tubing with varying lengths and diameters to achieve aortic resistances of 7, 13, 29, 65, and 82 mmHg cm^{-3} min^{-1} (calibrated at constant flow). Positive and negative *dP/dt* were determined on-line.
24. The care of all animals used in these studies was in accordance with institutional and IACUC guidelines.

Supported in part by grants from the Howard Hughes Medical Institute and NIH.

6 December 1995; accepted 8 March 1996